SEPARATING NON-LINEAR DEFORMATION AND ATMOSPHERIC PHASE SCREEN (APS) FOR INSAR TIME SERIES ANALYSIS USING LEAST-SQUARES COLLOCATION

S. Liu, R. F. Hanssen, S. Samiei-Esfahany, A. Hooper, and F. J. van Leijen

Mathematical Geodesy and Positioning, Faculty of Aerospace Engineering, Delft University of Technology, PO Box 5058, 2600GB, The Netherlands, {s.liu}{r.f.hanssen}{s.samieiesfahany}{f.j.vanLeijen}@tudelft.nl

ABSTRACT

We present a new method for separating ground deformation from atmospheric phase screen (APS) based on PSInSAR. By stochastic modeling of ground deformation and APS via their variance-covariance functions we can not only estimate the signals with the best accuracy but also assess the estimation accuracy using least-squares collocation [5]. We evaluate the APS estimated by our method and the APS obtained from a commonly used window-based filtering method [6] by comparing them to repeat-pass interferograms over ground surfaces outside the subsiding region of Mexico City. The comparison shows that our method results in a better estimation of APS than the filtering method which ignores the temporal variability of APS variance. Our method is desired when there are temporal gaps in a SAR time series. In such a case, the filtering method needs a large temporal window to suppress APS, which may lead to leakage from ground deformation to APS.

Key words: InSAR, atmospheric delay, least-squares collocation.

1. INTRODUCTION

Tropospheric delay, usually referred to as atmospheric phase screen (APS), imposes a serious practical limitation on accurate ground deformation analysis using InSAR. Methods which have been proposed to mitigate this nuisance can generally be grouped into two categories. The first category requires some ancillary data to estimate the APS independently. This estimation is subsequently subtracted from the interferometric phase. The ancillary data may originate from regional GPS networks [1], space-borne spectroradiometers such MERIS and MODIS [2], or numerical weather forecasting [3]. This category of mitigation methods is usually hampered by the measurement availability and spatial density, weather conditions (e.g., cloud and sunlight) or prediction reliability which prevent these methods from being generic solutions for APS mitigation.

The second, SAR-based, category attempts to estimate the APS directly, based on assumptions on its stochastic behavior and a time series of SAR images. Stochastically, two APSs are uncorrelated when their temporal baseline is larger than one day [4]. In general, these methods require a complete modeling of signals (e.g., ground deformation, APS, orbit errors, etc.,) embedded in the InSAR time series.

In this paper we introduce a new SAR based algorithm to estimate APS and ground deformation with the possible optimal accuracy from a time series of SAR images. Based on a-priori assumptions which are falsifiable in practice about the signals of interest, the optimal accuracy is proven by the least-squares collocation principle [5]. Although the algorithm is implemented for Persistent Scatterers InSAR (PSInSAR) [6], it can be adapted to other time series based approaches as well.

2. LEAST-SQUARES COLLOCATION AND VARIANCE-COVARIANCE ESTIMATION

In this section we elaborate on the developed algorithm which consists of two parts: least-squares collocation (LSC) and variance-covariance estimation. The basic observation model for LSC is a well known *trend-signal-noise* model used in many geoscience related studies [9]. A successful application of LSC requires a good modeling of the stochastic variates in the trend-signal-noise model. This topic is however beyond the framework of LSC in which the stochastic properties, e.g., variance-covariance functions, of the variates are assumed already known. Variance-covariance function estimation is discussed in section 2.2.

2.1. Least-squares collocation (LSC)

2.1.1. LSC applied to a time series per arc

Suppose N+1 SAR images from which N interferograms sharing a common master are formed and M+1 pix-

Proc. 'Fringe 2011 Workshop', Frascati, Italy, 19–23 September 2011 (ESA SP-697, January 2012)

els which have a low amplitude dispersion index [6] are selected from the N interferograms as Persistent Scatterer Candidates (PSC) [7]. These PSCs form a so-called *first-order* network in which their interferometric phases are unwrapped and tested for correcting unwrapping errors [8]. The unwrapped interferometric phase between a PSC p and a reference PSC r forms a spatial arc of the first-order network and can be modeled as:

$$\begin{aligned}\underline{\phi}^{\text{obs}}_{\text{p, r}} &= \underline{\phi}^{\text{defo}}_{\text{p, r}} + \phi^{\text{topo}}_{\text{p, r}} + \phi^{m,\text{aps}}_{\text{p, r}} + \phi^{m,\text{orb}}_{\text{p, r}} \\ &\quad -\underline{\phi}^{s,\text{aps}}_{\text{p, r}} - \underline{\phi}^{s,\text{orb}}_{\text{p, r}} + \underline{\phi}^{\text{noise}}_{\text{p, r}}, \end{aligned} \tag{1}$$

where $\underline{\phi}^{\text{obs}}_{\text{p, r}}$ is the unwrapped and tested interferometric phase serving as an observation, $\underline{\phi}^{\text{defo}}_{\text{p, r}}$ is the phase caused by ground deformation, $\phi^{\text{topo}}_{\text{p, r}}$ is the phase due to unmodeled topographic contribution, $\phi^{m,\text{aps}}_{\text{p, r}}$ and $\phi^{s,\text{aps}}_{\text{p, r}}$ are the APS of the master and a slave respectively, $\phi^{m,\text{orb}}_{\text{p, r}}$ and $\underline{\phi}^{s,\text{orb}}_{\text{p, r}}$ are the results of orbit uncertainties of the master and a slave respectively, $\underline{\phi}^{\text{noise}}_{\text{p, r}}$ accounts for a phase noise due to phase decorrelation and thermal noise. Here, we denote stochastic variables by underlines to distinguish them from deterministic variables. The deformation phase $\underline{\phi}^{\text{defo}}_{\text{p, r}}$ is denoted as a stochastic variable because we model the total deformation as the sum of a deterministic term which can be modeled by a linear function (e.g., a linear, quadratic or periodic trend) and a stochastic term which has a zero-mean and is second-order stationary in time, i.e., $\underline{\phi}^{\text{defo}}_{\text{p, r}} = \phi^{\text{defo, det}}_{\text{p, r}} + \underline{\phi}^{\text{defo, sth}}_{\text{p, r}}$. Moreover, $\phi^{m,\text{aps}}_{\text{p, r}}$ and $\phi^{m,\text{orb}}_{\text{p, r}}$ are also denoted as deterministic variables since they appear in every interferogram sharing a common master.

Following the discussion above, we model the time series of the arcs formed by PSCs p and r by a *trend-signal-noise* model which can be written in a matrix form as:

$$\Phi^{\text{obs}}_{\text{p, r}} = A\mathbf{x}_{p,r} + \underline{\mathbf{s}}_{p,r} + \underline{\mathbf{n}}_{p,r}, \tag{2}$$

where $\Phi^{\text{obs}}_{\text{p, r}}$ is an $N\times 1$ vector which contains the interferometric phases. $A\mathbf{x}_{p,r}$ is the temporal trend component in which $\mathbf{x}_{p,r}$ is an $n\times 1$ vector that contains unknown deterministic parameters, including coefficients of the linear function used to model the deterministic part of the deformation $\phi^{\text{defo, det}}_{\text{p, r}}$, the topographic contribution $\phi^{\text{topo}}_{\text{p, r}}$ and a component t which is the sum of $\phi^{\text{m, aps}}_{\text{p, r}}$, $\phi^{\text{m, orb}}_{\text{p, r}}$, i.e., $t = \phi^{\text{m, aps}}_{\text{p, r}} + \phi^{\text{m, orb}}_{\text{p, r}}$. The choice of the linear function to model $\phi^{\text{defo, det}}_{\text{p, r}}$ is arbitrary but usually depends on a priori assumptions/knowledge about the area under investigation. Assumptions which can be explicit or implicit are often inevitable in parameter estimation because many inverse problems such as the one described in Eq. (2) are inherently under-determined and ill-posed. Matrix A is a design matrix with N rows and n columns. If $\phi^{\text{det, defo}}_{\text{p, r}}$ can be modeled as a linear function of time (i.e., a constant velocity), then A is an $N\times 3$ matrix and has the form:

$$A = -\frac{4\pi}{\lambda}\begin{bmatrix} \frac{B^1_\perp}{r^m_x \sin\theta^m_x} & B^1_{\text{T}} & 1 \\ \frac{B^2_\perp}{r^m_x \sin\theta^m_x} & B^2_{\text{T}} & 1 \\ \cdots & \cdots & \cdots \\ \frac{B^N_\perp}{r^m_x \sin\theta^m_x} & B^N_{\text{T}} & 1 \end{bmatrix}, \tag{3}$$

where $B_\perp$ and B_{T} are the perpendicular and temporal baselines of an interferogram, λ is the radar wavelength, r^m_x is the range from the master sensor to the PSC p and θ^m_x is the local incidence angle. The first column of A relates $\phi^{\text{dem}}_{\text{p, r}}$ with the DEM error Δh_p and $-\frac{4\pi}{\lambda}$ is a range to phase converter.

The signal component $\underline{\mathbf{s}}_{p,r}$ is an $N\times 1$ vector which contains the stochastic part of ground deformation which is not modeled by the function model in $A\mathbf{x}_{p,r}$. We assume $\underline{\mathbf{s}}_{p,r}$ is second order stationary in time with a zero mean. The noise component $\underline{\mathbf{n}}_{p,r}$ is an $N\times 1$ vector which contains the phases due to slave APS, slave orbit errors and decorrelation and thermal noises. We assume $\underline{\mathbf{n}}_{p,r}$ is second order stationary and uncorrelated in time with a zero mean.

The best linear unbiased estimation (BLUE) of $\mathbf{x}_{p,r}$ is [9]:

$$\hat{\underline{\mathbf{x}}}_{p,r} = (A^T Q^{-1}_{\Phi\Phi} A)^{-1} A^T Q^{-1}_{\Phi\Phi} \Phi^{\text{obs}}_{\text{p, r}}, \tag{4}$$

and the best linear unbiased prediction (BLUP) of $\underline{\mathbf{s}}_{p,r}$ is [9]:

$$\hat{\underline{\mathbf{s}}}_{p,r} = Q^{p,r}_{ss} Q^{-1}_{\Phi\Phi} (\Phi^{\text{obs}}_{\text{p, r}} - A\hat{\underline{x}}_{p,r}), \tag{5}$$

where $Q_{\Phi\Phi}$ and $Q^{p,r}_{ss}$ are the variance-covariance matrices of $\Phi^{\text{obs}}_{\text{p, r}}$ and $\underline{\mathbf{s}}_{p,r}$ respectively. The BLUP of the noise component $\underline{\mathbf{n}}_{p,r}$ is:

$$\hat{\underline{\mathbf{n}}}_{p,r} = Q^{p,r}_{nn} Q^{-1}_{\Phi\Phi} (\Phi^{\text{obs}}_{\text{p, r}} - A\hat{\underline{x}}_{p,r}), \tag{6}$$

where $Q^{p,r}_{nn}$ is the variance-covariance of $\underline{\mathbf{n}}_{p,r}$. The prediction error $\underline{\epsilon}_s$ (i.e., $\hat{\underline{s}}_{p,r}$ - $\underline{s}_{p,r}$) of $\hat{\underline{\mathbf{s}}}_{p,r}$ can be evaluated by [9]:

$$\begin{aligned} Q^{p,r}_{\hat{\epsilon}_s\hat{\epsilon}_s} &= Q^{p,r}_{ss} - Q^{p,r}_{ss} Q^{-1}_{\Phi\Phi} Q^{p,r}_{ss} + \\ &\quad (Q^{p,r}_{ss} Q^{-1}_{\Phi\Phi} A) Q^{p,r}_{\hat{x}\hat{x}} (Q^{p,r}_{ss} Q^{-1}_{\Phi\Phi} A)^T, \end{aligned} \tag{7}$$

where $Q^{p,r}_{\hat{x}\hat{x}} = A Q^{-1}_{\Phi\Phi} A^T$.

2.1.2. LSC applied to spatial arcs per SAR acquistion

Till now, we have obtained the best prediction of $\hat{\underline{\mathbf{n}}}_{p,r}$ per slave for each arc time series (formed by a PSC p and the reference PSC r). Next, we are going to separate APS ($\underline{\phi}^{\text{aps}}_{p,r}$), orbit errors ($\underline{\phi}^{\text{orb}}_{p,r}$) per slave and phase noises ($\underline{\phi}^{\text{noise}}_{p,r}$) based on their spatial characteristics. Taking one slave acquisition as an example, the $\underline{\mathbf{n}}^k$ (k denotes the kth

slave acquisition) in space can be written as:

$$\underline{\mathbf{n}}^k = \begin{bmatrix} \underline{n}^k_{1,\,\mathrm{r}} \\ \cdots \\ \underline{n}^k_{\mathrm{p},\,\mathrm{r}} \\ \cdots \\ \underline{n}^k_{\mathrm{M},\,\mathrm{r}} \end{bmatrix} = - \begin{bmatrix} \underline{\phi}^{k,\mathrm{aps}}_{1,\,\mathrm{r}} + \underline{\phi}^{k,\mathrm{orb}}_{1,\,\mathrm{r}} + \underline{\phi}^{k,\mathrm{noise}}_{1,\,\mathrm{r}} \\ \cdots \\ \underline{\phi}^{k,\mathrm{aps}}_{\mathrm{p},\,\mathrm{r}} + \underline{\phi}^{k,\mathrm{orb}}_{\mathrm{p},\,\mathrm{r}} + \underline{\phi}^{k,\mathrm{noise}}_{\mathrm{p},\,\mathrm{r}} \\ \cdots \\ \underline{\phi}^{k,\mathrm{aps}}_{\mathrm{M},\,\mathrm{r}} + \underline{\phi}^{k,\mathrm{orb}}_{\mathrm{M},\,\mathrm{r}} + \underline{\phi}^{k,\mathrm{noise}}_{\mathrm{M},\,\mathrm{r}} \end{bmatrix}. \quad (8)$$

For the APS component $\underline{\phi}^{k,\,\mathrm{aps}}$, we model it in space as a spatial trend plus a spatial variation (signal) and if applicable a height-dependent component usually known as the atmospheric vertical stratification [4]. The spatial trend usually manifests itself as a long wavelength surface trend which has been observed from many ERS-1/2 tandem interferograms and it is the result of the large spatial extent of high and low pressure zones [4]. The spatial variation component is mainly caused by the high spatial variation of water vapor in the lower troposphere, i.e., turbulent mixing [4]. It is usually modeled as a zero mean stochastic process and its spatial characteristics are often modeled via a structural analysis [4]. The height dependent component is applicable when the variation of the land topography in the area of interest is significant (e.g., ≥ 1000 m)[3], it can often be modeled as a linear function of height [3]. The orbital phase term $\underline{\phi}^{k,\mathrm{orb}}$ usually presents in interferograms as surface phase ramps and can be sufficiently modeled as a surface trend over a typical spatial extent of 100 by 100 km [4]. Since $\underline{\phi}^{k,\mathrm{aps}}$and $\underline{\phi}^{k,\mathrm{orb}}$ share the common spatial characteristic (i.e., a long wavelength trend) it is not possible to separate them in practice without any external data. Finally, the phase noise term $\underline{\phi}^{k,\mathrm{noise}}$ is modeled as a white noise, i.e., uncorrelated in space and time, a norm distribution with a zero mean.

Based on the spatial characteristics of the signals and in analogue to Eq. (2) in time domain, we model $\underline{\mathbf{n}}^k$ per slave in space by a *trend-signal-noise* model as:

$$\underline{\mathbf{n}}^k = R\mathbf{y}^k + \underline{\nu}^k + \underline{\mu}^k, \quad (9)$$

where R is the spatial design matrix which has M rows and 4 columns, $\mathbf{y}^k$ is a 4 by 1 parameter vector which contains three coefficients for determining a surface trend caused by troposphere and orbit errors and one coefficient taking into account the vertical stratification as a linear function of height. $\underline{\nu}^k$ is a $M\times 1$ vector which contains the phase component due to the turbulent mixing and $\underline{\mu}^k$ is the noise component. The BLUE of $\mathbf{y}^k$ is given as:

$$\underline{\hat{\mathbf{y}}}^k = (R^T(Q^k_{nn})^{-1}R)^{-1}R^T(Q^k_{nn})^{-1}\underline{\mathbf{n}}^k, \quad (10)$$

where Q^k_{nn} is the spatial VCM of $\underline{\mathbf{n}}^k$. Therefore, the BLUE of the spatial trend (due to troposphere and orbit errors) and the vertical stratification can be obtained as: $R\underline{\hat{\mathbf{y}}}^k$. To separate the turbulent mixing component from the phase noise, we use BLUP:

$$\underline{\hat{\nu}}^k = Q^k_{\nu\nu}(Q^k_{nn})^{-1}\underline{\mathbf{n}}^k, \quad (11)$$

where $Q^k_{\nu\nu}$ is the VCM of $\underline{\nu}^k$ for the kth slave APS.

2.2. Variance-covariance function estimation

The method elaborated in section 2.1 requires a number of VCMs, namely $Q^{p,r}_{ss}$ in Eq. 5, $Q^{p,r}_{nn}$ in Eq. 6, Q^k_{nn} in Eq. 10 and $Q^k_{\nu\nu}$ in Eq. 11, to be known in advance. However, they are rarely known a priori in practice and therefore have to be estimated first from the the observations (i.e., unwrapped interferometric phases on PSCs). The stochastic ground deformation component $\underline{\mathbf{s}}$ usually shows an autocorrelation between SAR acquisitions over areas undertaking a progressive deformation. Therefore, $Q^{p,r}_{ss}$ is a full square matrix (N by N) which describes the temporal covariance of the deformation time series between the PSCs p and r and with respect to the master acquisition. To model $Q^{p,r}_{ss}$ we use a parametric approach which guarantees the estimated $\hat{Q}^{p,r}_{ss}$ is positive-definite and invertible [10]. The parametric approach regards $Q^{p,r}_{ss}$ as a realization of its variance covariance function (VCF). Typically used VCF models in practice are spheric, exponential and gaussian models [11], etc. Moreover, assuming that APS (including turbulent mixing, vertical stratification and spatial trend components), orbit errors and phase noise do not have an autocorrelation in time, then $Q^{p,r}_{nn}$ is a diagonal matrix and the elements in its main diagonal represent the sum of the variance of APS, orbit errors and phase noise. For APS, the variance depends on weather conditions, the spatial distance between p and r as well as the height difference between p and r. The more turbulent the weather, the longer distance between p and r and the larger height difference between p and r, the larger the APS variance will be and vice versa. For the orbit errors, its variance only depends on the distance between p and r. We estimate $Q^{p,r}_{ss}$ and $Q^{p,r}_{nn}$ by restricted maximum likelihood estimator (RMLE) given in [10]. When the input data for the estimator has a normal distribution its estimates will have the minimum estimation error variance [10].

In space domain, applying the error propagation law [9] to Eq. (9) we have:

$$Q^k_{nn} = Q^k_{\nu\nu} + Q^k_{\mu\mu}, \quad (12)$$

where $Q^k_{\mu\mu}$ is the spatial VCM of the phase noise $\underline{\mu}^k$ in the kth interferogram, assuming $\underline{\nu}$ is uncorrelated with $\underline{\mu}$ in space. Since $\underline{\nu}$ is spatially correlated but $\underline{\mu}$ is not, $Q^k_{\nu\nu}$ is therefore a full square matrix (M by M) and $Q^k_{\mu\mu}$ is a diagonal matrix with the same size. Same as the modeling of $Q^{p,r}_{ss}$ we use the parametric approach to model $Q^k_{\nu\nu}$. Analyses based on ERS1/2 tandem interferograms suggest that VCFs from the Matérn-family [12] are appropriate [4]. To estimate $Q^k_{\mu\mu}$, we use the method described in [7].

3. LEAST-SQUARES COLLOCATION APPLIED TO MEXICO CITY

To evaluate the algorithm in section 2 we carry out a case study over Mexico City using 45 ASAR images (track

255, frame 3216) acquired between 2002 and 2008. The master image was acquired on 31-DEC-2004. In total 2576 pixels having an amplitude dispersion index lower than 0.22 are selected as PSCs over a 40 by 40 km crop centered at the urban area of the city and the PSC density is about 1.6 PSC/km^2. These PSCs form a so-called *first-order* network in which their interferometric phases are unwrapped and tested for inconsistency [7]. To model the ground deformation in time we use a quadratic function model and a hole effect variance-covariance model for its deterministic and stochastic components respectively. We choose the hole effect model because we suspect the area of interest may experience seasonal deformation due to seasonal variations of underground water. Since the urban area is relatively flat ($\Delta h_{\max} < 500$ m), the possible vertical stratification is therefore not taken into account in our analysis.

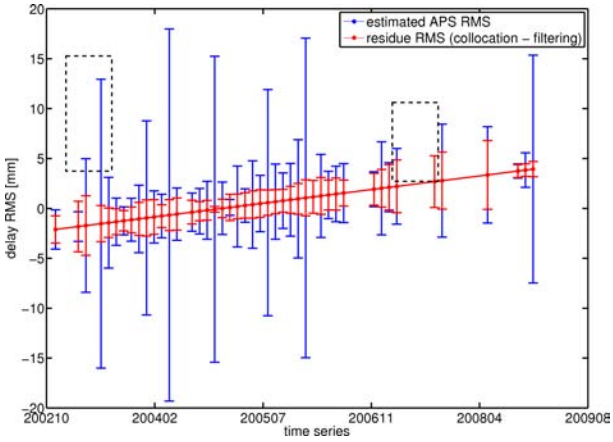

Figure 1. APS RMS in delays (mm). Blue: estimated APS RMS per acquisition by the collocation method. Red: RMS of the difference between APS estimates by the collocation and window-based filtering (1-year Gaussian window) methods. The black rectangles include the SAR pairs used to form interferograms in Figs. 2 and 3. Note, the RMS of the difference is relatively large at acquisitions where there are acquisition gaps and when the APS variances are relatively large during days having a more turbulent weather.

Figure 1 shows the estimated APS RMS per acquisition by our collocation method as well as the RMS of the difference between APS estimates per acquisition made by the collocation method and a commonly used window-based filtering method [6]. A large RMS of the difference means a large discrepancy between the estimates from the two methods. As we can see from the figure, the RMS of the difference is relatively large at acquisitions where there are acquisition gaps and when the APS variances are relatively large during days having a more turbulent weather. To evaluate the two methods we compare some of their results against several coherent repeat-pass interferograms over ground surfaces outside the subsiding region of the city. The APS estimates on 20-JUN-2003 and 11-APR-2003 are shown in Fig. 2 and the estimates on 7-SEP-2007 and 16-MAR-2007 are shown in Fig. 3. Both figures show that atmospheric anomalies visible in the repeat-pass interferograms are better estimated by the collocation method than the filtering method based on a 1-year Gaussian window. After increasing the window length from 1-year to 3-year, the filtering method gives more or less the same results as the collocation method. This is because a large temporal window will include more acquisitions into filtering and result in more suppression of APS which is temporal uncorrelated. The collocation method, however, suppress APS more effectively by weighted least-squares, i.e., low weights are given to the acquisitions which have large APS variances and vice versa.

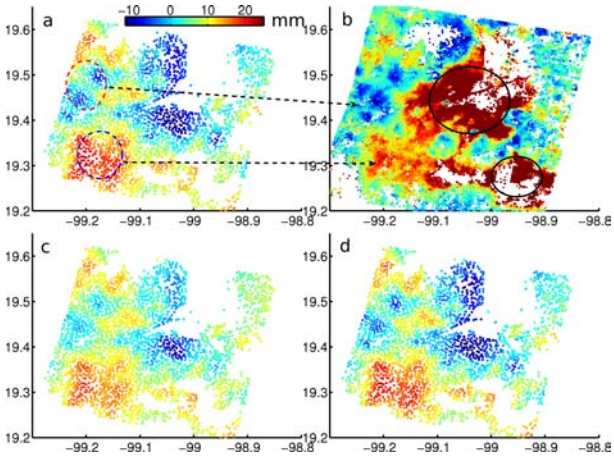

Figure 2. Interferogram on 20-JUN-2003 and 11-APR-2003. a) APS estimated by the collocation method on PS pixels. b) unwrapped interferogram by repeat-pass interferometry. c) APS estimated by the filtering method using a 1-year Gaussian temporal window. d) APS estimated by the filtering method using a 3-year Gaussian temporal window. Atmospheric anomalies visible in the repeat-pass interferogram are better estimated by the collocation method, see the sub-region highlighted by circles. The subsiding urban region is highlighted by black circles. The color-bar unit is in mm. X-axis: longitude, Y-axis: latitude.

Regarding deformation estimation, we do not have ground truth for validation. Instead, we plot two PS deformation time series in Fig. 4. The two PSs are from two sub-region highlighted in Figs. 2 and 3 respectively. From Fig. 4 we can see that the influence of uncompensated APS on the deformation time series as well as an over-smoothing effect caused by using a filtering window whose length is likely larger than the possible correlation length of the deformation. The collocation method, however, does not need to specify a window length and it estimates the correlation length of the deformation via its temporal variance-covariance function from the unwrapped phase time series. If the variance-covariance matrix is estimated accurately, the estimated deformation should have the best accuracy and the accuracy can be assessed via the estimated variance-covariance matrix, see error bars in Fig 4.

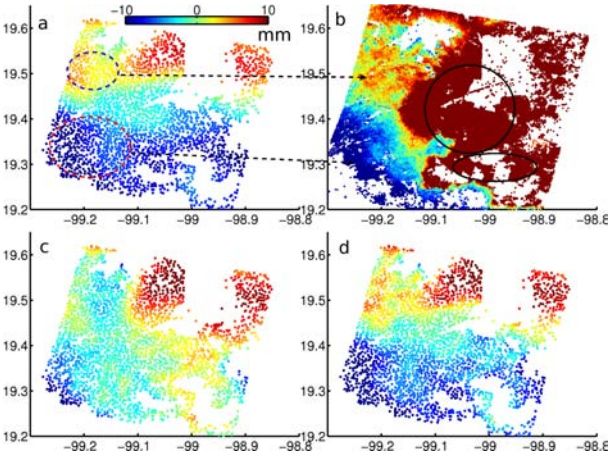

Figure 3. Interferogram on 7-SEP-2007 and 16-MAR-2007. a) APS estimated by the collocation method on PS pixels. b) unwrapped interferogram by repeat-pass interferometry. c) APS estimated by the filtering method using a 1-year Gaussian temporal window. d) APS estimated by the filtering method using a 3-year Gaussian temporal window. Atmospheric anomalies visible in the repeat-pass interferogram are better estimated by the collocation method, see the sub-region highlighted by dashed circles. The subsiding urban region is highlighted by black circles. The color-bar unit is in mm.

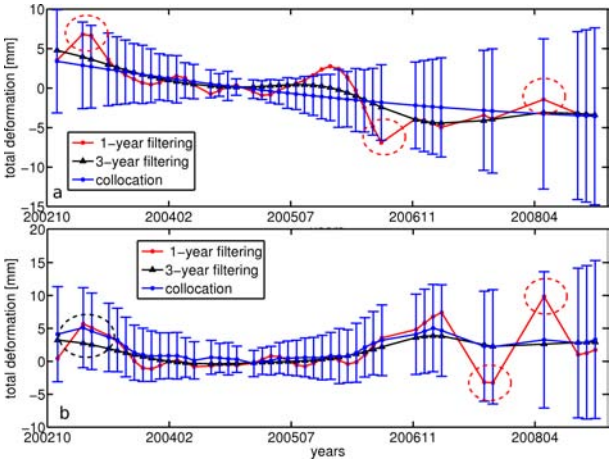

Figure 4. Time series of total ground deformation. a) One PS point selected from the region highlighted by the dashed red circle in Fig. 2. b) Another PS point selected from the region highlighted by the dashed red circle in Fig. 3. The error bars indicate the estimated accuracy of the deformation estimates. The dashed red circles indicate the influence of uncompensated APS on deformation estimation using the filtering method based on a 1-year Gaussian temporal window (see Figs. 2 and 3). The dashed black circle indicates an over-smoothing effect on the deformation time series when a 3-year Gaussian temporal window is used.

4. CONCLUSION

In this paper, we introduce a new method for separating ground deformation from atmospheric phase screen (APS) based on PSInSAR. We evaluate the APS estimated by our method and the APS obtained from a commonly used filtering method by comparing them to repeat-pass interferograms over ground surfaces outside the subsiding region of Mexico City. By taking into account the temporal variability of APS variance per acquisition our method is able to estimate APS more accurately than the filtering method which ignores the variability and requires a sufficient number of images to smooth out APS. Moreover, when there are temporal gaps in a SAR time series, a large temporal window is needed to suppress APS. However, it many over smooth the ground deformation when the deformation has a temporal correlation shorter than the window length.

REFERENCES

[1] S. Williams, Y. Bock, and P. Fang, "Integrated satellite interferometry: Tropospheric noise, GPS estimates and implications for interferometric synthetic aperture radar products," *Journal of Geophysical Research*, vol. 103, no. B11, pp. 27,051–27,067, 1998.

[2] Z. Li, J.-P. Muller, P. Cross, P. Albert, J. Fischer, and R. Bennartz, "Assessment of the potential of MERIS near-infrared water vapour products to correct ASAR interferometric measurements," *International Journal of Remote Sensing*, vol. 27, pp. 349–365, 2006.

[3] S. Liu, A. Mika, and R. Hanssen, "On the value of high-resolution weather models for atmospheric mitigation in SAR interferometry," in *International Geoscience and Remote Sensing Symposium, Cape Town, South Africa, 12–17 July 2009*, p. 4 pp, 2009.

[4] R. F. Hanssen, *Radar Interferometry: Data Interpretation and Error Analysis*. Dordrecht: Kluwer Academic Publishers, 2001.

[5] H. Moritz, "Interpolation and prediction of gravity and their accuracy," Tech. Rep. 24, Inst Geod Phot Cart, Ohio State University, Columbus, USA, 1962.

[6] A. Ferretti, C. Prati, and F. Rocca, "Nonlinear subsidence rate estimation using permanent scatterers in differential SAR interferometry," *IEEE Transactions on Geoscience and Remote Sensing*, vol. 38, pp. 2202–2212, Sept. 2000.

[7] B. M. Kampes, *Displacement Parameter Estimation using Permanent Scatterer Interferometry*. PhD thesis, Delft University of Technology, Delft, the Netherlands, Sept. 2005.

[8] B. M. Kampes and R. F. Hanssen, "Ambiguity resolution for permanent scatterer interferometry," *IEEE Transactions on Geoscience and Remote Sensing*, vol. 42, pp. 2446–2453, Nov. 2004.

[9] P. J. G. Teunissen, "Least-squares prediction in linear models with integer unknowns," *Journal of Geodesy*, vol. 81, pp. 565–579, 2007.

[10] P. K. Kitanidis, "Parametric estimation of covariances of regionalized variables," *Water Resources Bulletin*, vol. 23, pp. 557–567, Aug. 1987.

[11] A. G. Journel and C. J. Huijbregts, *Mining Geostatistics*. London: Academic Press, 1978.

[12] M. L. Stein, *Interpolation of Spatial Data; Some Theory for Kriging*. Springer Series in Statistics, Springer, 1999.

[13] P. Berardino, G. Fornaro, R. Lanari, and E. Sansosti, "A new algorithm for surface deformation monitoring based on small baseline differential SAR interferograms," *IEEE Transactions on Geoscience and Remote Sensing*, vol. 40, no. 11, pp. 2375–2383, 2002.